



## Effective removal of Pb(II), Cd(II) and Zn(II) from aqueous solution by a novel hyper cross-linked nanometer-sized chelating resin

Manal El Hefnawy<sup>a,\*</sup>, A.F. Shaaban<sup>b</sup>, H.A. ElKhawaga<sup>a</sup>

<sup>a</sup> Faculty of Engineering (Shoubra), Benha University, Benha, Egypt

<sup>b</sup> Chemistry Department, Faculty of Science, Benha University, Benha, Egypt



### ARTICLE INFO

#### Keywords:

Hyper-cross-linked  
Nanometer-sized chelating resin  
Kinetics  
Isotherms  
Thermodynamics

### ABSTRACT

A novel hyper cross-linked nanometer-sized chelating resin (HCNSCR) was synthesized and characterized by Fourier transform infrared spectroscopy. The thermal stability of the prepared HCNSCR was also defined using thermogravimetric analysis (TGA). The surface morphology and the porous structure of the resin were studied by scanning electron microscopy (SEM), transmission electron microscopy (TEM) and Brunauer- Emmett –Taller (BET). The presence of Zn(II), Cd(II), and Pb(II) with the prepared resin was confirmed by using EDX (Energy Dispersive-X- ray spectroscopy). The sorption capacity of the synthesized HCNSCR towards the three metal ions and the factors affecting their elimination from aqueous solutions like pH effect, metal ion concentration, temperature and contact time were demonstrated by the batch method. The results illustrated that the sorption capacity of the synthesized HCNSCR towards Pb(II), Cd(II), and Zn(II) ions were 1.2, 1 and 0.9 (mmol. g<sup>-1</sup>) respectively, also the adsorption process was highly pH depended where the optimum PH for pb(II), Cd(II), and Zn(II) was 5.5, 6, 6.3 respectively. The experimental data and the kinetic data of adsorption isotherms indicated that the adsorption process was well fitted to the Langmuir isotherm and the pseudo-second-order kinetic model expresses the adsorption process, also from thermodynamic parameters it was cleared that the adsorption process was spontaneous and endothermic and the process marked with increase in randomness furthermore the resin was regenerated with a minor loss of adsorption capacity after 5 cycles of adsorption and usage.

### 1. Introduction

Contamination of water resources is a prevalent occurrence. Hazardous metals pollution is among the most serious environmental issues that danger human being all over the world with the acceleration of industrialization and urbanization [1,2]. Heavy metals such as Pb, Zn, Cd, Cu, Hg, etc. could pose a severe threat to humans' health as they cannot be degraded by microorganisms once they are released into the environment; so, they are accumulated biologically in the food chain [3]. The most poisonous of these metals are: lead, cadmium, and zinc. Lead can cause central nervous system damage, renal and hepatic failure, in addition to impairing basic cellular function [4].

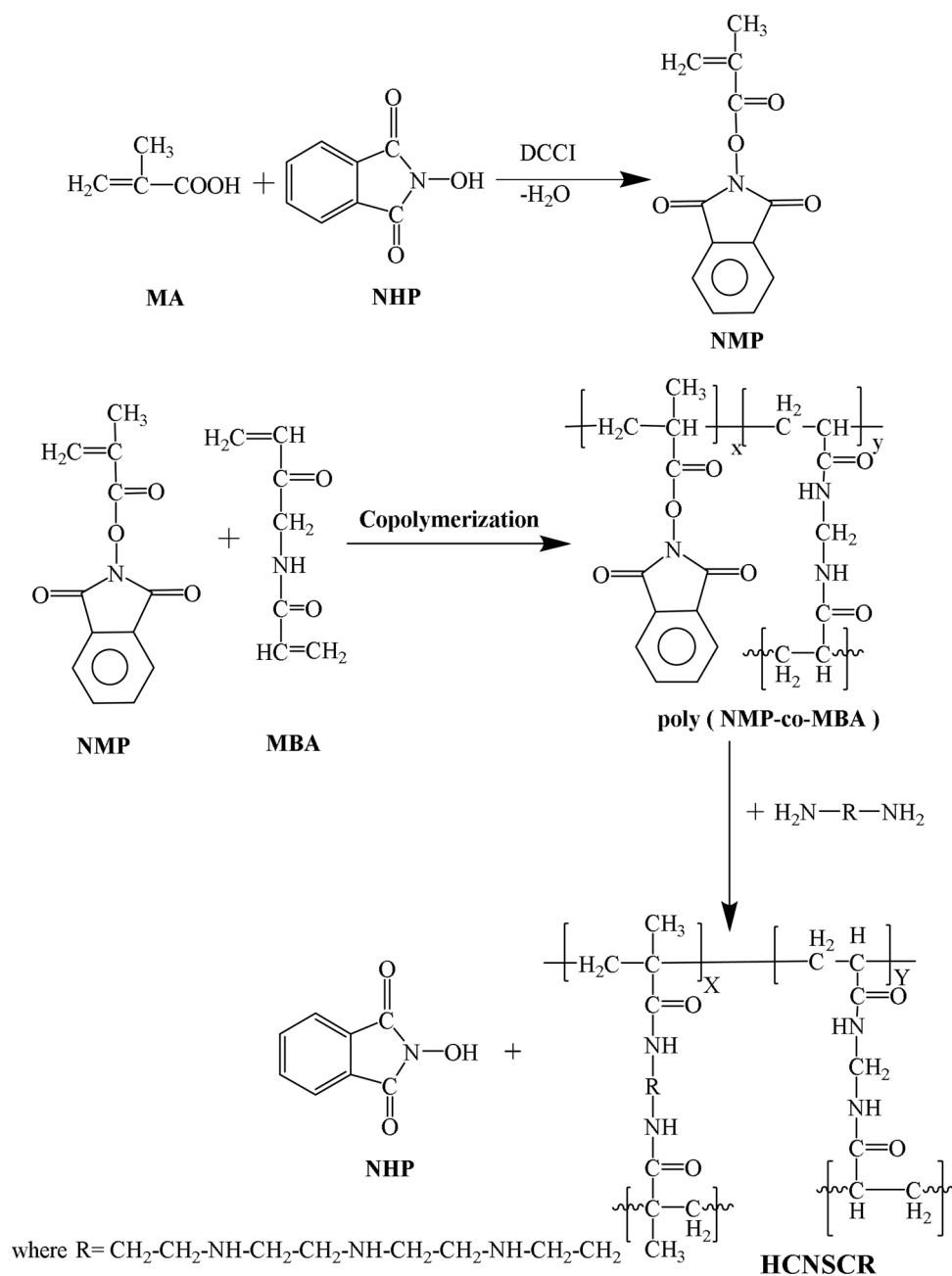
Cadmium exposure results in the degeneration of bones and liver damage in addition to being carcinogenic [5]. Zinc element is essential to a human being because it helps in organizing several biological processes and, it has a vital role in many physiological functions, but high amounts of Zinc can cause several health problems, such as: vomiting, stomach spasms, anemia, and skin irritation [6]. Therefore, the removal of heavy metals from water is of great importance and has

drowned tremendous attention.

Several methods have been used recently for extracting heavy metals, such as liquid-liquid extraction, electrolytic concentration, precipitation, adsorption, membrane filtration and ion exchange [7–9], adsorption is the most favorable due to its relatively easy procedures and abundance of diverse organic sorbents including chelating functional groups [10–21]. Currently, different kinds of nanomaterials are used widely as adsorbents, including activated carbon, clay, metal oxides, graphene materials and polymers [22–32]. Nanomaterials have significantly large surface area which is an essential property for the required sorbent; this explains the increasing interest of nanomaterials improvement by many researchers in the past decades [33–35]. Polymer adsorbents are indeed suitable for applications as potential adsorbents due to the perfect skeleton strength, adjustable surface functional groups, feasible regeneration, degradable properties and environmental harmlessness [36–40]. However, the low adsorption capacity and selectivity still need improvements for practical application. One of the effective strategies to improve the adsorption performance of polymeric materials is the surface functionalization of

\* Corresponding author.

E-mail addresses: [manalehefnawy@yahoo.com](mailto:manalehefnawy@yahoo.com) (M. El Hefnawy), [afshaaban@hotmail.com](mailto:afshaaban@hotmail.com) (A.F. Shaaban), [elkhawaga@gmail.com](mailto:elkhawaga@gmail.com) (H.A. ElKhawaga).



Scheme 1. Schematic illustration of the preparation process of HCNSCR.

polymers to obtain polymer-based composites.

In our current work, a novel hyper cross-linked nanometer-sized chelating resin (HCNSCR) was synthesized and identified by different spectral techniques. The adsorption capacity of the synthesized HCNSCR for Pb (II), Cd (II) and Zn (II) ions were demonstrated by the batch method where the factors influencing their elimination from aqueous solutions were explained as a function of pH of the solution, concentration of metal ions, contact time and temperature.

## 2. Experimental and characterization techniques

### 2.1. Materials

Methacrylic acid, *N*-hydroxyphthalimide (NHP) and *N,N*-dicyclohexylcarbodiimide (DCC) were purchased from Merck Co, Germany. Methylenebisacrylamide (MBA), tetraethylenepentamin (TEPA), polyvinyl alcohol (PVA) and benzoyl peroxide were purchased from Sigma-

Aldrich Co., USA, where all the solvents which were utilized had been purified before using and were of reagent grade.

### 2.2. Synthesis of nanometer-sized chelating resin (HCNSCR)

NMP (*N*-methacryloylphthalimid) was synthesized as mentioned in our prior work [41,42]. Poly (NMP-co-MBA) was synthesized according to our prior work [43] utilizing a suspension polymerization technique. HCNSCR was prepared through the addition of 6.47 mL of TEPA to a mixture of 10 mL toluene and 0.5 g of poly (NMP-co-MBA) under a mechanical stirrer (1200 rpm) and reflux for 48 h at 100 °C. The produced ultrafine precipitate of HCNSCR was obtained by centrifuging and then washed using both acetone and ethanol to eliminate any liberated NHP, a residue of toluene, or TEPA then put in a vacuum dryer at 60 °C to yield 0.5978 g of HCNSCR after purification.

### 2.3. Characterization of the adsorbent

The prepared NMP, poly (NMP-co-MBA) and HCNSCR were recognized by FTIR using Shimadzu 8201 PC in KBr phase.

TGA of the prepared HCNSCR was detected by SDT Q600 V20.9 Build 20, USA in nitrogen atmosphere with a flowing rate of 20 mL/min in temperature between room temperature and 1000 °C.

Brunauer–Emmett–Taller (BET) and BJH methods were used through N<sub>2</sub> adsorption-desorption methods to determine the HCNSCR porosity utilizing N<sub>2</sub> as the adsorbent at 77.35 K. A model NOVA 3200 automated gas sorption system (Quanta chrome, USA) was used for the measurement.

QUANTA FEG scanning electron microscopy SEM at 60,000 magnifications and 20KV accelerating voltage also TEM transmission electron microscopy JEOL [JEM-1230 electron microscopy] was utilized to study the morphology and particle size of HCNSCR.

### 2.4. Sorption of metal ions by the batch method

All experiments were achieved using 0.1 g of HCNSCR in 100 mL of single-metal ion solution at 25 °C (except the temperature experiments at 35, 45, and 55 °C) in a controlled shaker at 250 rpm and few drops of NaOH and/or HCl solutions were used for the adjustment of the pH. HCNSCR was then separated from the metal ions solution using the centrifuge and Hitachi atomic absorption Z-6100 polarized Zeeman was used to study the metal ion concentration in the supernatant solution. The below equation was used to calculate the average value of the equilibrium adsorption capacity ( $q_e$ )

$$q_e = \frac{(C_o - C_e)V}{W} \quad (1)$$

Where  $C_o$  and  $C_e$  the initial and final metal ion solutions concentrations respectively ( $\text{mmol}\cdot\text{L}^{-1}$ ),  $V$  is the volume of metal ions solution (L) and  $W$  the weight of the dry resin (g).

## 3. Results and discussion

HCNSCR was synthesized by three steps illustrated in Scheme 1. NHP reacts with MA in the presence of DCC as dehydrating agents to prepare NMP, in the second step the poly (NMP-co-MBA) was prepared by copolymerization of NMP with MBA as across linking agent by suspension polymerization. Finally HCNSCR was obtained by reaction of poly (NMP-co-MBA) with tetraethelenepentamin (TEPA). The prepared chelating resins particle size depends on the cross-linked agent (MBA) amount in the oil phase. A nanometer-sized chelating resin was obtained with a diameter ranging from 63.14 to 95.79 nm in case of 40 % MBA.

### 3.1. Resin characterization

#### 3.1.1. FTIR and thermal stability of the synthesized resin

FTIR spectra of the prepared monomer (NMP) illustrated in the prior work [41,42], FTIR spectra of poly (NMP-co-MBA) and HCNSCR were shown in (Fig. 1a and b). Fig. 1a showed a band at  $3423\text{ cm}^{-1}$  due to N–H of amide group, a band at  $2934\text{ cm}^{-1}$  of C–H aliphatic, three significant bands at  $1742$ ,  $1655$  and  $1531\text{ cm}^{-1}$  corresponding to C=O of imides, amide (I) and amide (II) groups, respectively, band at  $696\text{ cm}^{-1}$  corresponding to the four adjacent hydrogen atoms of the benzene ring and band at  $930\text{ cm}^{-1}$  for N–O. IR spectrum of HCNSCR (Fig. 1b) showed a band at  $3424\text{ cm}^{-1}$  related to NH, a significant band at  $2927\text{ cm}^{-1}$  of C–H aliphatic, bands at  $1650$  and  $1546\text{ cm}^{-1}$  characteristic for the stretching frequency of C=O of amide (I) and amid (II) respectively.

The thermal stability of the HCNSCR was defined using TGA as shown in Fig. 2 the degradation of the resin occurred within three steps. The first step refers to water vapor and volatile materials loss existing in

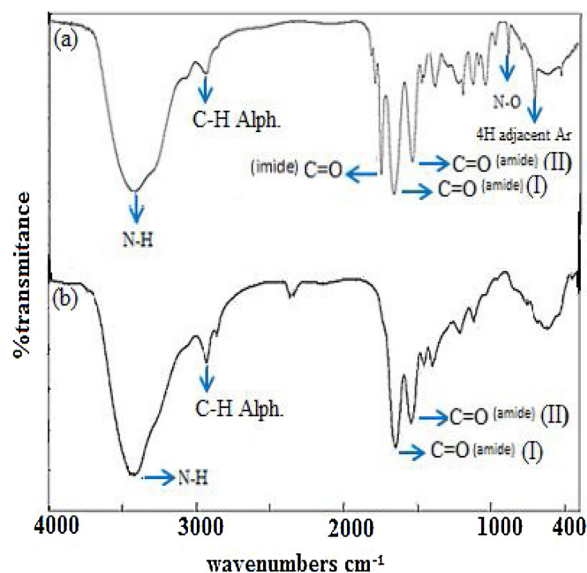


Fig. 1. FT-IR spectra of (a) poly (NMP-co-MBA) and (b) HCNSCR.

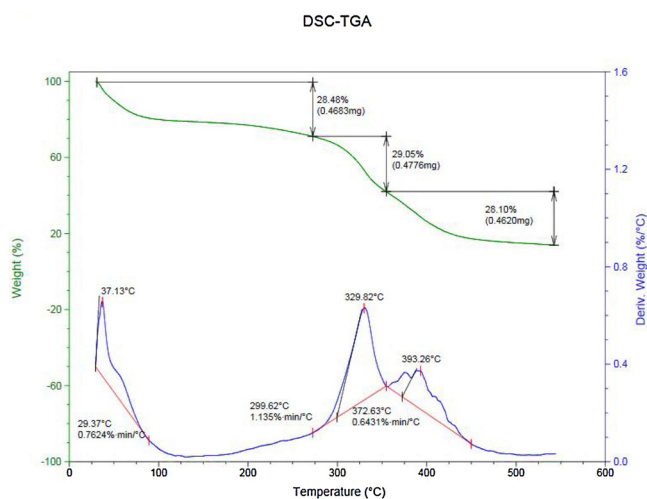


Fig. 2. TGA of the prepared HCNSCR.

exterior surface and interior pores or cavities of the resin which occurred at 29–268 °C with a partial weight loss of 28.48 %. HCNSCR represents a new class of hydrophilic hyper cross-linked polymer which has a higher surface area ( $335\text{ m}^2\text{ g}^{-1}$ ) and mesoporous structure (2.882 nm) favor the adsorption of polar compounds and volatile organic compounds from water sample [44,45]. The second stage which represents the degradation of grafted functional groups occurred at 268–353 °C with a partial weight loss of 29.05 %. The third stage occurred at 353–526 °C with a partial weight loss of 28.10 % referred to the decomposition of modified cross-linking agents and polymer chain.

#### 3.1.2. Surface area

The BJH pore volume, average pore diameter and BET surface area for HCNSCR were determined and the results are shown in Table 1

**Table 1**  
Porous structure parameters of HCNSCR.

Parameters	HCNSCR
BET surface area ( $\text{m}^2/\text{g}$ )	335
BJH desorption average pore diameter (nm)	2.882
BJH desorption cumulative volume of pores ( $\text{cm}^3/\text{g}$ )	0.1600

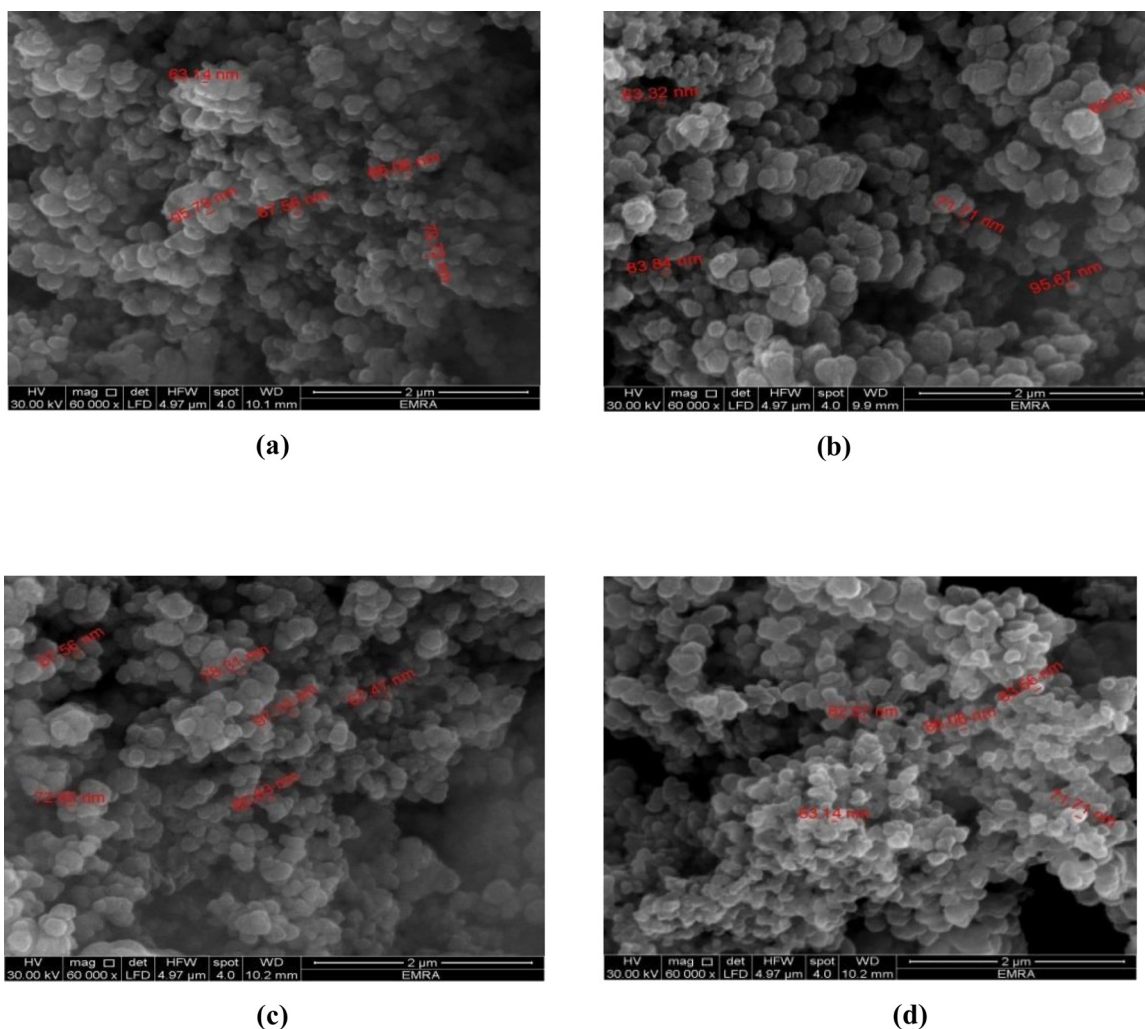


Fig. 3. SEM images of a HCNSCR b HCNSCR-Pb, c HCNSCR-Cd and d HCNSCR-Zn with magnification 60,000 $\times$ .

which illustrate that the HCNSCR had pore volume of 0.16 (cm<sup>3</sup> g<sup>-1</sup>) and pore diameter of 2.882 nm which to be considered mesoporous structure [46].

### 3.1.3. Scanning electron microscopy-EDX

The morphology of the resin before the sorption of metal ions is shown in Fig. 3a, which illustrated the synthesized resin particle size in nano-scale with a diameter ranging from 63.14 to 95.79 nm. Fig. 3(b, c, and d) shows the prepared resin particle size still in nano-scale after the metal ions sorption. The particles of HCNSCR before and after adsorption do not appear like isolated particles owing to their agglomeration. However, these nano-scale particles offer favorable sorption processes due to their large surface area [47].

EDX spectra for HCNSCR and its metal complexes are shown in Fig. 4 which confirms the presence of lead, cadmium, and zinc with the prepared HCNSCR. The resin with Pb(II), Cd(II) and Zn(II) ions shows distinct signals at 1.8, 2.4, 2.7, 10.55, 12.6, 3.15, 3.33, 3.55, 1, 8.6, and 9.7 keV respectively, the level of the signals detected was adequate for supplying the homogeneous distribution of Pb, Cd, and Zn elements at the sorbent surface qualitatively (not quantitatively). The percentage (in mass) of Pb, Cd, and Zn was 17.46 %, 11.9 % and 6.99 %, respectively.

### 3.1.4. Transmission electron microscopy

Fig. 5 shows the TEM image at 200 nm for the synthesized HCNSCR, which demonstrated the synthesized resin particle size in nano-scale with an average diameter of 76.68 nm.

## 3.2. Uptake of metal ions utilizing the batch technique of HCNSCR

### 3.2.1. Optimum pH of metal ions uptake

The optimum pH of the sorption of metal ions in a pH range from 1 to 6.5 was demonstrated it was proved from Fig. 6 that as the pH increased the sorption capacity of the metal ions increased since the nanoparticle surface charge becomes more negative at higher pH consequently the electrostatic attraction between the resin and metal ion increases. The optimum pH for Pb (II), Cd (II) and Zn (II) was 5.5, 6 and 6.3, respectively. After this optimum value, the sorption efficiency is almost unchanged as all the metal ions precipitated as metal (II) hydroxide.

$M^{+2} + OH \rightarrow M(OH)_2$  The chelation models of the HCNSCR with metal ions based on TEPA and MBA moieties are demonstrated in Schemes 2 and 3 respectively. It was cleared that MBA repeating units are helpful to increase metal ions sorption [43] as the oxygen and nitrogen atoms in the two amide groups in it are included in the chelation with the metal ions.

### 3.2.2. Initial concentration of the metal ions and equilibrium isotherm models

The effect of the initial concentration on metal ions adsorption in a concentration of metal ion solution ranging from 1 to 13 (mmol L<sup>-1</sup>) at the optimum pH and 25 °C was shown in Fig. 7 which illustrated that the adsorption of the metal ions on the resin increases as the initial concentration of it increases and the optimum concentrations of metal

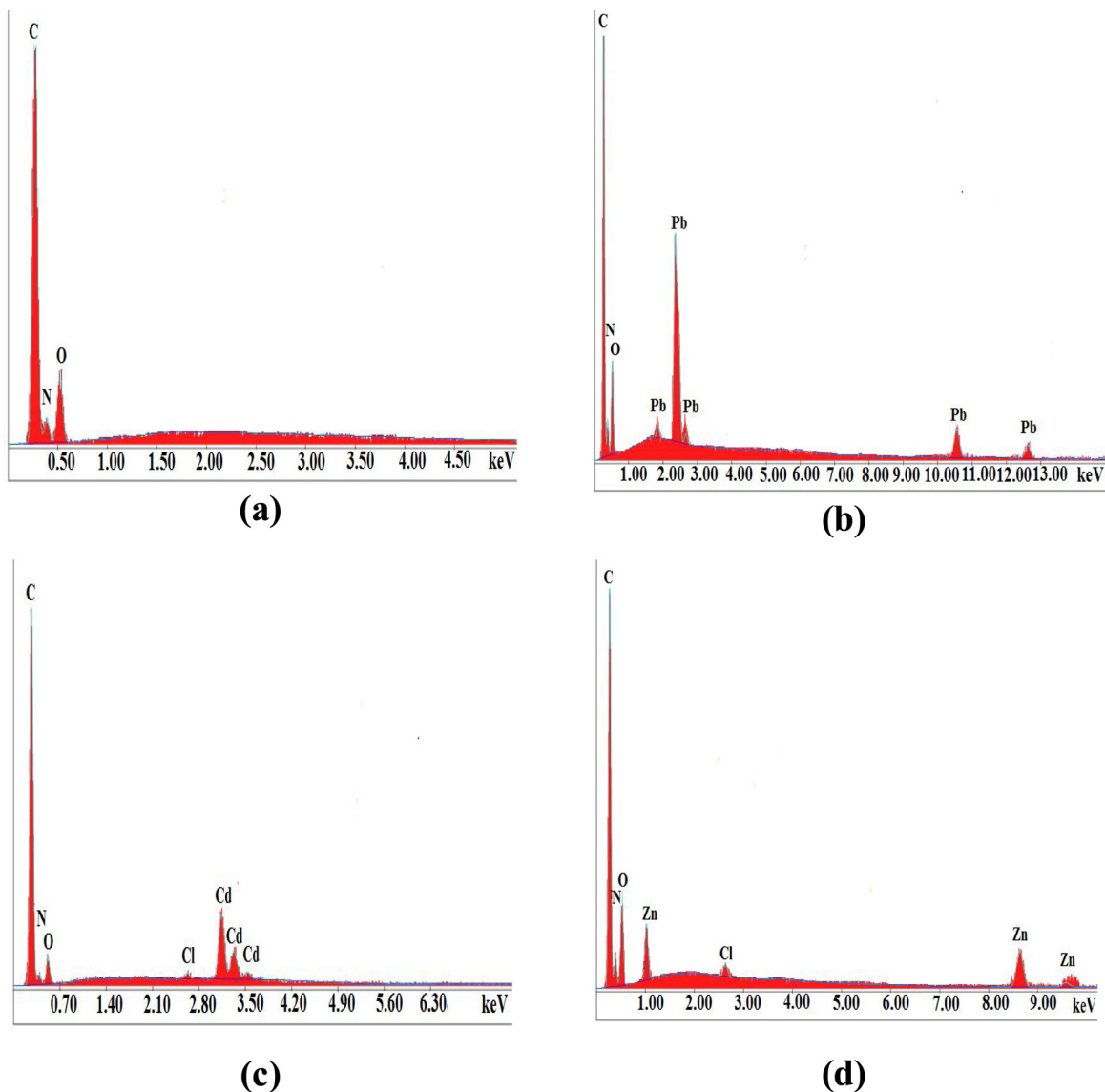


Fig. 4. EDX images of (a) HCNSCR, (b) HCNSCR-Pb, (c) HCNSCR-Cd and (d) HCNSCR-Zn.

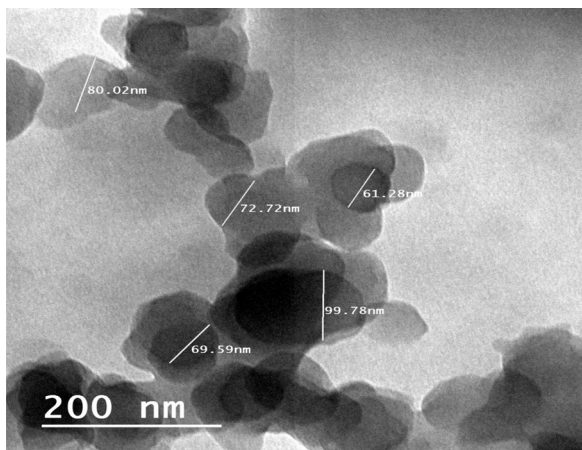


Fig. 5. TEM image of HCNSCR.

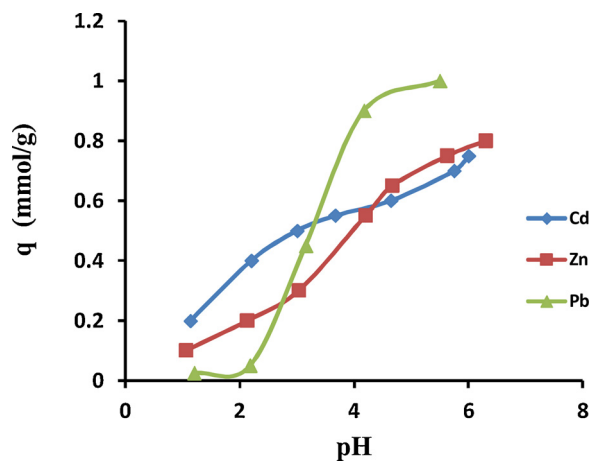
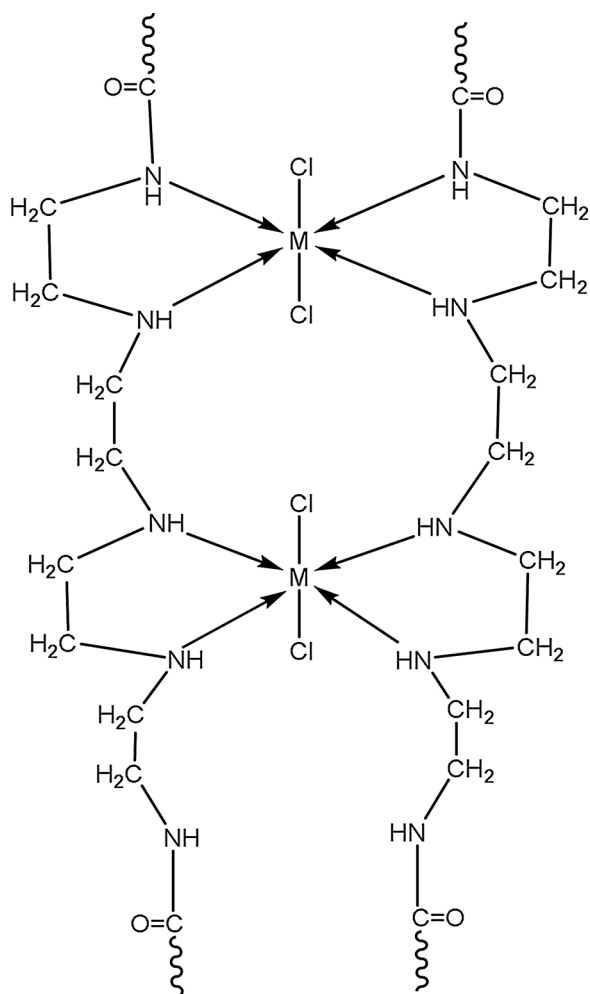
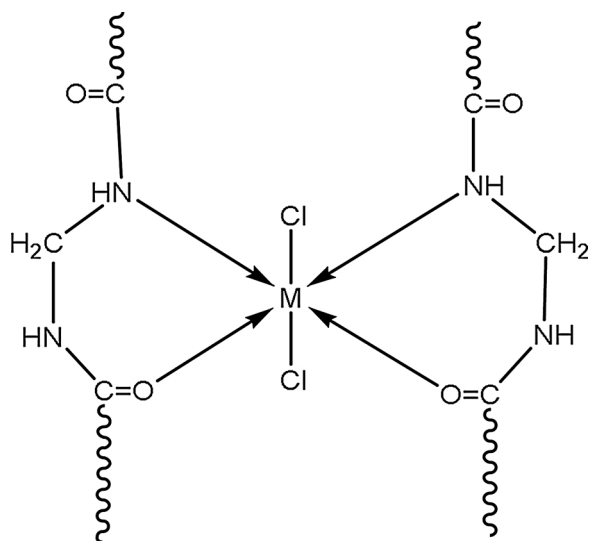


Fig. 6. Effect of pH on the uptake of metal ions.



**Scheme 2.** Schematic illustration for the chelation process of HCNSCR with the metal ions based on TEPA moieties.



**Scheme 3.** Schematic illustration for the chelation process of HCNSCR with the metal ions based on MBA moieties.

ions for Pb(II), Cd(II) and Zn(II) are 10.3, 10.2 and 9.3 (mmol/L) respectively, also by comparing the hydrated ionic radius of Zn(II) (4.30 Å), Cd (II) (4.26 Å) and Pb(II) (4.01 Å) it was cleared that the smaller the hydrated ionic radius the greater the adsorption of metal

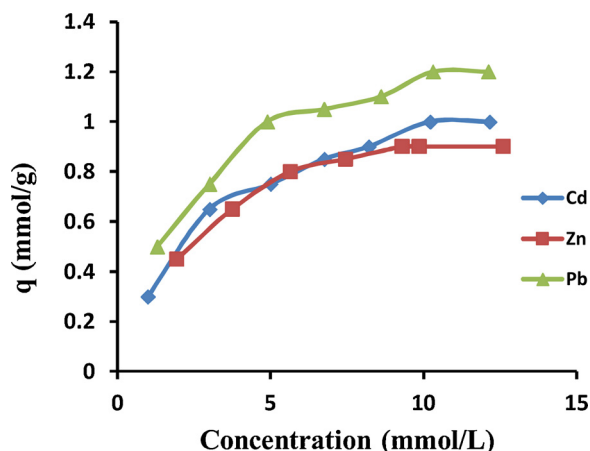


**Fig. 7.** Effect of initial metal ions concentration on the sorption capacity.

ions [48,49] therefore Pb (II) was the most adsorbed by HCNSCR as it has the smallest hydrated ionic radius accordingly, it can simply take place in the pores of the chelating resin (average pore diameter of HCNSCR equal to 2.882 nm). A comparison of HCNSCR with different types of adsorbents reported in literatures is shown in Table 2.

The metal ions sorption capacity was specified using the three isotherm models usually used i.e. Langmuir, Freundlich, and Temkin isotherm represented by the following three equations respectively [58–63]:

$$\frac{C_e}{q_e} = \frac{C_e}{Q_{\max}} + \frac{1}{K Q_{\max}} \quad (2)$$

$$\log q_e = \frac{1}{N} \log C_e + \log K_F \quad (3)$$

$$q_e = B \ln k_T + B \ln C_e \quad (4)$$

$Q_{\max}$  (mmol g<sup>-1</sup>) is the saturated single layer adsorption capacity; K (L/mmol) is the Langmuir adsorption constant concerned to the desirability of binding sites,  $K_F$  is the Freundlich constant (index of adsorption capacity) and N is also Freundlich Constant that concerned of the level of heterogeneity of the surface site.  $B$  (Jmol<sup>-1</sup>) is Temkin constant which is correlated to the sorption heat and  $K_T$  is the equilibrium binding constant. The results of Langmuir were represented in Table 3.

The dimensionless constant separation factor ( $R_L$ ) which reflects the essential characteristics of the Langmuir model can be determined from the following equation:

$$R_L = \frac{1}{1 + K C_0} \quad (5)$$

By plotting  $R_L$  versus  $C_0$  as shown in Fig. 8 the calculated values of  $R_L$  were between zero and one detect that the adsorption process of the metal ions onto HCNSCR is favorable [64].

The values of  $K_F$  and N in Freundlich model are also calculated from the intercept and the slope by plotting  $q_e$  versus  $\log C_e$  and these constant were collected in Table 3, the value of N in Freundlich isotherm explained the nature of isotherm  $N = 0$  irreversible,  $N > 1$  is unfavorable or  $0 < N < 1$  is favorable as shown from Table 3 the value of N was between zero and one for the three metal ions indicated that the metal ions adsorption on HCNSCR was favorable. The  $R^2$  (correlation coefficient) obtained for the plots of the three isotherm illustrated the validity of the three isotherm models for the adsorption process however, the higher value of  $R^2$  obtained for the Langmuir model show that the experimental data were more favorable with this isotherm model suggesting a monolayer coverage of metal ion onto the resin surface [65].

**Table 2**

Comparison of maximum sorption capacity of HCNSCR with those of some other chelating resins reported in the literature for the adsorption of Pb (II), Cd (II) and Zn (II).

Adsorbents	Metal ions	Sorption capacity (mmol/g)	Conditions	Ref
Manganese oxide-coated sand,(MOCS),	Pb(II) and Zn(II)	0.65 and 1.78	pH=6 27 °C	[50]
Magnetic chlorapatite nanoparticles (MNCLAP)	Zn(II),Cd(II)and Pb(II)	1.1769, 1.1022 and 1.1546	pH = 5 ± 0.1 25 ± 1 °C	[51]
Fe <sub>2</sub> O <sub>3</sub> -ceramistite (FOC)	Pb(II) and Zn(II)	0.08 and 0.11	pH = 5 25 ± 0.5 °C	[52]
Amidoxime modified poly(acrilonitrile-co-acrylic acid)	Cd(II) and Pb(II)	0.18 and 0.6	pH=9 25 °C	[53]
Rice Husk	Zn(II) and Pb (II)	0.3 and 0.003	pH 4.4 25 ± 1 °C	[54]
olive stone activated carbon (COSAC)	Cd(II) and Pb(II)	0.53 and 0.54	pH = 5 30°C	[55]
Na-montmorillonite (Na-Mt) and Ca-montmorillonite (Ca-Mt)	Pb(II),Cd(II) and Zn(II)	0.262, 0.204, 0.151	pH = 4.08	[56]
Poly(amidoamine)modified GO	Pb(II) and Zn(II)	0.0513, and 0.2024	pH = 5-6 25 °C	[57]
HCNSCR	Pb(II),Cd(II) and Zn(II)	1.2, 1 and 0.9	pH = 5.5, 6.0 and 6.3 25 °C	This work

### 3.2.3. Adsorption kinetics

Variations of adsorption capacity ( $q_e$ ) were plotted vs time to examine the effect of contact time between an aqueous solution of metal ions and HCNSCR on the adsorption of metal ions. It was obvious from Fig. 9 that the metal ions sorption increases as the contact time increases till it reaches equilibrium after 3 h among two phases. Accordingly, this optimum equilibrium time was used to study the kinetic mechanism which controls the adsorption process.

To examine the kinetic process; the commonly used models of Lagergren's pseudo-first- order; pseudo-second order and intraparticle diffusion were utilized [66–68]. The linear shape of the first order rate equation by Lagergren and Svenska [66] is shown in Eq. (6)

$$\log(q_e - q_t) = \log q_e - \left(\frac{k_1}{2.303}\right)t \quad (6)$$

The pseudo-second-order kinetic model of Ho [67] can be presented as follow:

$$\frac{t}{q_t} = \frac{1}{k_2 q_e^2} + \left(\frac{1}{q_e}\right)t \quad (7)$$

Where  $q_e$  (mmol. g<sup>-1</sup>) and  $q_t$  (mmol. g<sup>-1</sup>) the quantity of metal ions adsorbed at equilibrium and at time t respectively,  $K_1$  is the Lagergren rate constant of adsorption (min<sup>-1</sup>) and  $K_2$  is the pseudo-second- order rate constant.

Sorption reactions are multistep reactions contain bulk diffusion, thin film diffusion, intra-particle diffusion and adsorbate /adsorbent interaction (chemical or physical). The stirring of the adsorption solution makes the bulk diffusion effect very weak and can be neglected; accordingly, the rate- determining step may be intra-particle diffusion and/or adsorbate /adsorbent interaction. Batch experiments were treated according to the Weber- Morris model in Eq. (8) [68].

$$q_t = k_{id} t^{0.5} \quad (8)$$

Where  $k_{id}$ , is the intraparticle diffusion rate constant (mmol. g<sup>-1</sup>/min<sup>0.5</sup>). The constants of the previously mentioned three models were shown in Table 4. The kinetic data in the table indicated that the sorption procedure is described will by pseudo-second- order kinetic model, and by plotting  $q_e$  vs  $t^{0.5}$  the plot showed multi-linearity signifying several steps for the metal ions sorption [69] as shown in Fig. 10

**Table 3**

Parameters of Langmuir, Freundlich and Temkin isotherm for adsorption of metal ions on HCNSCR.

Metal ion	Langmuir isotherm			Freundlich isotherm			Temkin isotherm		
	Q <sub>max</sub> (mmol/g)	K	R <sup>2</sup>	N	K <sub>f</sub>	R <sup>2</sup>	K <sub>T</sub>	B	R <sup>2</sup>
Pb(II)	1.379	0.6126	0.9962	0.3413	0.5657	0.9697	7.5391	0.2782	0.9832
Cd(II)	1.200	0.4496	0.9951	0.4312	0.3869	0.9598	4.7913	0.2558	0.9921
Zn(II)	1.074	0.5334	0.9953	0.3496	0.4213	0.9315	5.1841	0.2339	0.9571

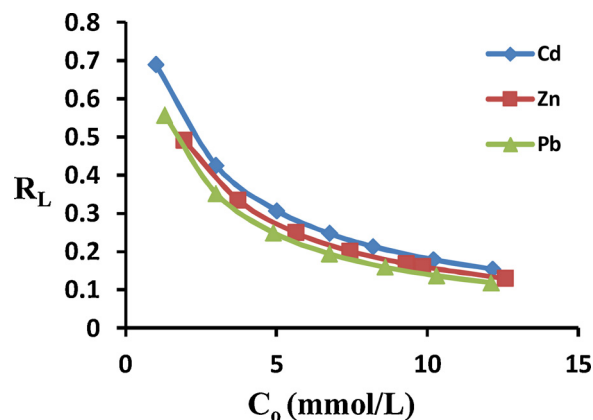


Fig. 8. Variation of adsorption intensity (RL) with initial concentration (Co).

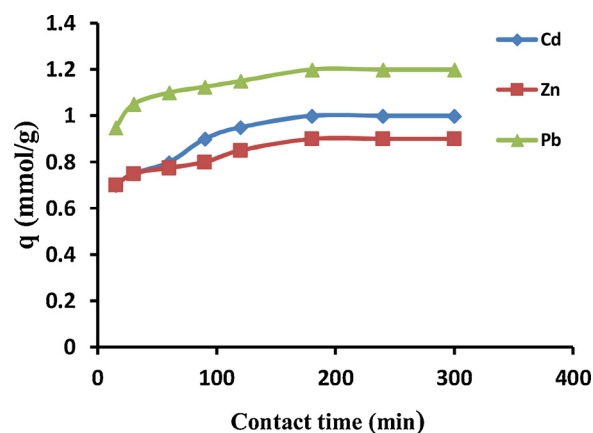


Fig. 9. Effect of shaking time on the sorption capacity.

### 3.2.4. Thermodynamics of adsorption

To calculate the thermodynamic parameters; the adsorption tests were done at three various temperatures (35, 45 and 55 °C). The equilibrium distribution coefficient for sorption procedure  $k_d$  was illustrated by Eq. (9) [70].

**Table 4**  
First-order, second-order, and intra particle diffusion rate constants.

Metal ion	Pseudo-first order kinetics			Pseudo-second-order kinetics			Intra particle diffusion	
	q <sub>e</sub> (mmol/g)	K <sub>1</sub> (min <sup>-1</sup> )	R <sup>2</sup>	q <sub>e</sub> (mmol/g)	K <sub>2</sub> (min <sup>-1</sup> )	R <sup>2</sup>	K <sub>id</sub> (mmol g <sup>-1</sup> min)	R <sup>2</sup>
Pb(II)	0.262	0.0143	0.9609	1.226	0.1369	0.999	0.0172	0.8633
Cd(II)	0.433	0.0168	0.9576	1.046	0.0784	0.998	0.0244	0.9033
Zn(II)	0.238	0.0117	0.9321	0.929	0.1188	0.999	0.0157	0.9345

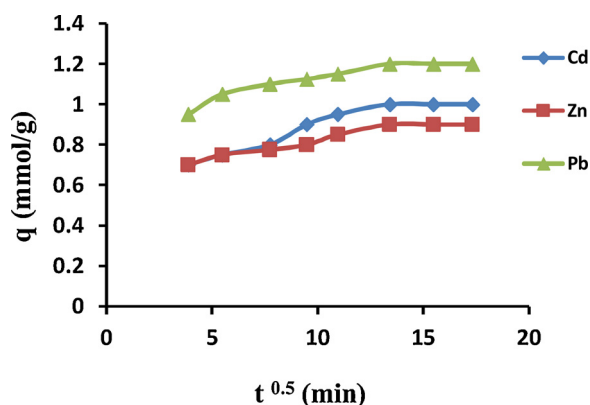


**Fig. 10.** Plot of Weber-Morris intra particle diffusion model for the metal ions adsorption on HCNSCR.

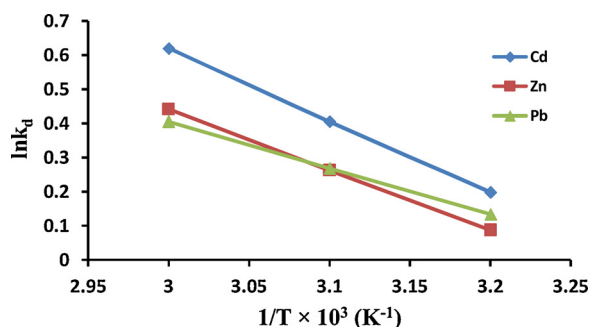


**Fig. 11.** Plot of lnkd vs 1/T for metal ions sorption on HCNSCR.

**Table 5**  
Thermodynamic parameters for the metal ions sorption onto the chelating resin.

Metal ion	-ΔG <sub>ads</sub> <sup>o</sup> (KJ/mol)			ΔH <sub>ads</sub> <sup>o</sup> (KJ/mol)	ΔS <sub>ads</sub> <sup>o</sup> (J/mol)	R <sup>2</sup>
	328 K	318 K	308 K			
Pb(II)	1.106	0.709	0.342	11.303	37.276	1.000
Cd(II)	1.692	1.072	0.509	17.531	57.741	0.9999
Zn(II)	1.204	0.694	0.223	14.732	47.860	1.000

$$k_d = \frac{(C_o - C_e)}{C_e} \times \frac{V}{W} \quad (9)$$

Where C<sub>o</sub> and C<sub>e</sub> are the initial and equilibrium concentration of the metal ions (mmol.L<sup>-1</sup>), V, and W are the volume of the solution in (L) and the weight of the HCNSCR in (g).

ΔG<sub>ads</sub><sup>o</sup> (free energy change of adsorption) was calculated using Eq. (10):

$$\Delta G_{ads}^o = -RT \ln k_d \quad (10)$$

ΔH<sub>ads</sub><sup>o</sup> and ΔS<sub>ads</sub><sup>o</sup> of the adsorption process can be calculated from the slope and the intercept, respectively by plotting lnK<sub>d</sub> against 1/T as in Eq. (11) and Fig. 11

$$\ln k_d = \frac{\Delta S_{ads}^o}{R} - \frac{\Delta H_{ads}^o}{RT} \quad (11)$$

The values of the three thermodynamic parameters (ΔG<sub>ads</sub><sup>o</sup>, ΔH<sub>ads</sub><sup>o</sup>, and ΔS<sub>ads</sub><sup>o</sup>) were shown in Table 5 Where the positive values of ΔH<sub>ads</sub><sup>o</sup> confirm that the adsorption process is an endothermic furthermore, the positive values of ΔS<sub>ads</sub><sup>o</sup> is due to the increase of the randomness of the system as a result of the loss of water of hydration through the sorption procedure [71,72], while the negativity of ΔG<sub>ads</sub><sup>o</sup> assumed that the adsorption process was spontaneous. The increase in negativity of ΔG<sub>ads</sub><sup>o</sup> as the temperature increase proves that the process is more proper at high temperatures.

### 3.2.5. Regeneration of the adsorbent

0.2 M HNO<sub>3</sub> at 25 °C was used to study the regeneration of loaded HCNSCR with Pb(II), Cd(II) and Zn(II) through several successive adsorption-desorption cycles. The data indicate that the sorption capacity minimized from 100 % to 93 % over 5 cycles.

## 4. Conclusion

A new nanometer chelating resin was synthesized and identified by Fourier transformed infrared spectroscopy and the thermal stability was defined also using TGA. The surface morphology and porous structure of the resin were studied by using several spectral methods. The synthesized resin particle was found to be in the nanoscale before the sorption process with a diameter ranging from 63.14 to 95.79 nm and also after the sorption process it remained within the nanoscale. The EDX spectra confirmed the homogeneous distribution of the three metal ions at the resin surface moreover, the adsorption efficiency of the nanoresin was investigated by the batch technique which confirmed that the nanoresin exhibits good adsorption capacity towards Pb(II), Cd(II) and Zn(II) from their aqueous solution according to the following order Pb(II) > Cd(II) > Zn(II). The effects of pH, initial metal ions concentration, adsorption time and temperature were also studied. In addition to studying the adsorption isotherm which confirmed the validity of the three models (Langmuir, Freundlich and Temkin) to the adsorption process; however, the higher correlation value (R<sup>2</sup> is 0.9962) demonstrates that the adsorption process was will fitted to Langmuir isotherm suggesting that the adsorption was monolayer and the kinetic data is well described by the pseudo-second-order model. The thermodynamic parameter indicates that the sorption process endothermic and spontaneous with marked increase in randomness. Furthermore, the reusability of the resin indicated that it might have potential application in treating heavy metal pollution in water.

### CRediT authorship contribution statement

**Manal El Hefnawy:** Conceptualization, Visualization, Writing - review & editing. **A.F. Shaaban:** Supervision, Investigation, Formal analysis. **H.A. ElKhwaga:** Methodology, Validation.

### Declaration of Competing Interest

The authors declare that they have no known competing financial

interests or personal relationships that could have appeared to influence the work reported in this paper.

## References

- [1] T. Yao, T. Cui, J. Wu, Q. Chen, S. Lu, K. Sun, Preparation of hierarchical porous polypyrrol nanoclusters and their application for removal of Cr (VI) ions in aqueous solution, *Polym. Chem.* 2 (2011) 2893–2899.
- [2] G. Zhao, X. Huang, Z. Tang, Q. Huang, F. Niu, X. Wang, Polymer -based nanocomposite for heavy metal ions removal, *Polym. Chem.* 9 (2018) 3562–3582.
- [3] M. Cheraghi, B. Lorestani, N. Yousefi, Effect of waste water on heavy metal accumulation in Hamedan Province vegetables, *Int. J. Bot.* 5 (2009) 190–193.
- [4] R. Naseem, S.S. Tahir, Removal of Pb (II) from aqueous solution by using bentonite as an adsorbent, *Water Res.* 35 (2001) 3982–3986.
- [5] X. Zhu, T. Song, Z. Lv, G. Ji, High efficiency and low-cost  $\alpha\text{Fe}_2\text{O}_3$  nano particles coated volcanic rock for Cd(II) removal from wastewater, *Process Saf. Environ. Prot.* 104 (2016) 273–381.
- [6] N. Oyaro, O. Juddy, E.N.M. Murago, E. Gitonga, The content of Pb, Cu, Zn and Cd in meat in Nairobi, Kenya, *Int. J. Food Agric. Environ.* 5 (2007) 119–121.
- [7] M.A. Tofghy, T. Mohammadi, Adsorption of divalent heavy metal ions from water using nanotube sheet, *J. Hazard. Mater.* 185 (2011) 140–147.
- [8] H. Deligz, E. Erdem, Comparative studies on the solvent extraction of transition metals cations by calixarene, phenol and ester derivatives, *J. Hazard. Mater.* 154 (2008) 29–32.
- [9] H. Bessbousse, T. Rhlalou, J.F. Verchere, L. Lebrun, Removal of heavy metals ions from aqueous solution by filtration, *J. Membr. Sci.* 307 (2008) 249–259.
- [10] B.L. Rivas, B. Quilodran, E. Quiroz, Trace metal ion retention properties of cross-linked poly (4-vinylpyridine) and poly (acrylic acid), *J. Appl. Polym. Sci. Symp.* 92 (2008) 2908–2916.
- [11] W.D. Henry, D. Zhao, A.K. Sengupta, C. Lang, Preparation and characterization of a new class of polymeric ligand exchangers for selective removal of trace contaminants from water, *React. Funct. Polym. Res.* 60 (2004) 109–120.
- [12] A. Nastasovic, S. Jovanovc, D. Dordevic, A. Onjia, D. Jakovljevic, T. Novakovic, Metal sorption on macro porous poly (GMA-co-EGDMA) modified with ethylene diamine, *React. Funct. Polym.* 58 (2004) 139–147.
- [13] A. Baraka, P.J. Hall, M.J. Heslop, Preparation and characterization of melamine-formaldehyde-DTPA chelating resin and its use as an adsorbent for heavy metals removal from wastewater, *React. Funct. Polym.* 67 (2007) 585–600.
- [14] S. Catedo, A. Gianguzza, D. Muralove, A. Pettignano, Pd adsorption by a novel activated carbon –alginate composite material –a kinetics and equilibrium study, *Int. J. Biol. Macromol.* 92 (2016) 769–778.
- [15] V. Neagu, I. Bunia, C. Luca, Organic ion exchangers' synthesis and their behavior in the retention of some metal ions, *Macromol. Symp.* 235 (2006) 136–142.
- [16] A. Denizli, N. Sanli, B. Garipcan, S. Patir, G.K. Isancak, Methacryloyl amidoglutamic acid incorporated porous poly (methyl methacrylate) beads for heavy-metal removal, *Ind. Eng. Chem. Res.* 43 (2004) 6095–6101.
- [17] M.J. Zohuriaan Mehr, A. Pourjavadi, M. Salehi Rad, Modified cmc. 2. novel carboxymethylcellulose-based poly (amidoxime) chelating resin with high metal sorption capacity, *React. Funct. Polym.* 61 (2004) 23–31.
- [18] A.F. Shaaban, D.F. Fadel, A.A. Mahmud, M.A. Elkomy, S.M. Elbahy, Synthesis of a new chelating resin bearing amidoxime group for adsorption of Cu(II), Ni(II) and Pb (II) by batch and fixed-bed column methods, *J. Environ. Chem. Eng.* 2 (2014) 632–641.
- [19] A.F. Shaaban, D.F. Fadel, A.A. Mahmoud, M.A. Elkomy, S.M. Elbahy, Removal of Pb (II), Cd(II), Mn(II) and Zn(II) using iminodiacetate chelating resin by batch and fixed bed column, *Desalin. Water Treat.* 51 (2013) 5526–5536.
- [20] A.F. Shaaban, D.F. Fadel, A.A. Mahmoud, M.A. Elkomy, S.M. Elbahy, synthesis and characterization of dithiocarbamate chelating resin and its adsorption performance towards Hg(II), Cd(II) and Pb(II) by batch and fixed-bed column methods, *J. Environ. Chem. Eng.* 1 (2013) 208–217.
- [21] A.F. Shaaban, T.Y. Mohamed, D.F. Fadel, N.M. Bayomi, removal of Ba(II) and Sr(II) ions using modified chitosan beads with bidentate amidoxime moieties by batch and fixed column methods, *J. Desal. Water Treat.* 82 (2017) 131–145.
- [22] X. Ren, J. Li, X. Tan, X. Wang, Comparative study of graphene oxide, activated carbon and carbon nanotubes as adsorbents for copper decontamination, *Dalton Trans.* 42 (2013) 5266–5274.
- [23] G. Zhao, H. Zhang, Q. Fan, X. Ren, J. Li, Y. Chen, X. Wang, Sorption of copper(II) onto super-adsorbent of bentonite-polyacrylamide composites, *J. Hazard. Mater.* 173 (2010) 661–668.
- [24] M. Verma, I. Tyag, R. Chandra, V.K. Gupta, Adsorption removal of Pb(II) ions from aqueous solution using nanoparticles synthesized by sputtering method, *J. Mol. Liq.* 225 (2017) 936–944.
- [25] X. Tan, M. Fang, X. Ren, H. Mei, D. Shao, X. Wang, Synergistic effect of humic and fulvic acids on Ni removal by the calcined Mg/Al layered double hydroxide, *Environ. Sci. Technol.* 48 (2014) 13138–13145.
- [26] X. Tan, Q. Fan, X. Wang, B. Grambow, Eu(III) sorption to TiO<sub>2</sub> (anatase and rutile): batch, XPS, and EXAFS studies, *Environ. Sci. Technol.* 43 (2009) 3115–3121.
- [27] X. Tan, M. Fang, J. Li, Y. Lu, X. Wang, Adsorption of Eu(III) onto TiO<sub>2</sub>: effect of pH, concentration, ionic strength and soil fulvic acid, *J. Hazard. Mater.* 168 (2009) 458–465.
- [28] C. Chen, X. Wang, Sorption of Th(IV) to silica as a function of humic/fulvic acid, ionic strength, electrolyte type, *Appl. Radiat. Isot.* 65 (2007) 155–163.
- [29] G. Zhao, J. Li, X. Ren, C. Chen, X. Wang, Few layered graphene oxide nanosheets as superior sorbents for heavy metal ion pollution management, *Environ. Sci. Technol.* 45 (2011) 10454–10462.
- [30] Y. Huang, J. Li, X. Chen, X. Wang, Application of conjugated polymer-based composites in wastewater purification, *RSC Adv.* 4 (2014) 62160–62178.
- [31] R. Hu, D. Shao, X. Wang, Graphene oxide polypyrrol composites for highly selective enrichment of U (VI) from aqueous solutions, *Polym. Chem.* 5 (2014) 6207–6215.
- [32] D. Shao, Z. Jiang, X. Wang, J. Li, Y. Meng, Plasma induced grafting carboxymethyl cellulose on multiwalled carbon nanotubes for the removal of UO<sub>2</sub> + 2, *J. Phys. Chem. B* 113 (2009) 860–864.
- [33] F. Ge, M. Li, H. Ye, B. Zhao, Effective removal of heavy metal ions Cd<sup>2+</sup>, Zn<sup>2+</sup>, Pb<sup>2+</sup>, Cu<sup>2+</sup> from aqueous solution by polymer-modified magnetic nanoparticles, *J. Hazard. Mater.* 211 (2012) 366–372.
- [34] L. Cumbal, A.K. Sen Gupta, Arsenic removal using polymer-supported hydrated iron (III) oxide nanoparticles: role of donnan membrane effect, *Environ. Sci. Technol.* 39 (2005) 6508–6515.
- [35] K. Zargoosh, H. Abedini, A. Abdolmaleki, M.R. Molavian, Effective removal of heavy metal ions from industrial wastes using thiosalicylhydrazide-modified magnetic nanoparticles, *Ind. Eng. Chem. Res.* 52 (2013) 14944–14954.
- [36] B. Pan, B. Pan, W. Zhang, L. Lv, Q. Zhang, S. Zheng, Development of polymeric and polymer-based hybrid adsorbents for pollutants removal from water, *Chem. Eng. J.* 151 (2009) 19–29.
- [37] X. Zhao, L. Lv, B. Pan, W. Zhang, S. Zhang, Q. Zhang, Polymer supported nanocomposites for environmental application, *Chem. Eng. J.* 170 (2011) 381–394.
- [38] H.N.M.E. Mahmud, A.O. Huq, R. Binti Yahya, The removal of heavy metal ions from wastewater /aqueous solution using polypyrrol-based adsorbents, *RSC Adv.* 6 (2016) 14778–14791.
- [39] D. Wang, X. Wang, Y. Xu, J. Li, J. Xu, X. Wang, Polyaniline nanorods dotted on graphene oxide nanosheet as a novel super adsorbent for Cr(IV), *Dalton Trans.* 42 (2013) 7854–7858.
- [40] H.N.M.E. Mahmud, A.O. Huq, R. Binti Yahya, The removal of heavy metal from wastewater/aqueous solution using polypyrrol based adsorbents, *RSC Adv.* 6 (2016) 14778–14791.
- [41] A.F. Shaaban, M.M.H. Arief, A.A. Khalil, N.N. Messina, 2-poly-N-acryloyl oxy-and -N-methacryloyloxyphthalimide as activated drug-binding matrices, *Acta Polym. Sin.* 39 (1988) 143–148.
- [42] A.A. Khalil, Exchange reactions of poly-2-(N-phthalimido) ethyl acrylate with hydroxyl and amino compounds, *J. Appl. Polym. Sci.* 99 (2006) 2258–2262.
- [43] A.F. Shaaban, A.A. Khalil, Mohamed Radwan, H.A. Manal El Hefnawy, Elkhawag, synthesis, characterization and application of a novel nanometer-sized chelating resin for removal of Cu(II), Co(II) and Ni(II) ions from aqueous solutions, *J. Polym. Res.* 24 (2017) 165–176.
- [44] C. Long, Y. Li, W. Yu, A. Li, Adsorption characteristics of water vapor on the hyper-cross-linked polymeric adsorbent, *Chem. Eng. J.* 180 (2012) 106–112.
- [45] D. Bratkovska, N. Fontanals, F. Borrull, P.A.G. Cormack, D.C. Sherrington, R.M. Marce, Hydrophilic hyper-cross-linked polymeric sorbents for the solid-phase extraction of polar contaminants from water, *J. Chromatogr. A* 1217 (2010) 3238–3243.
- [46] A. Gurses, M. Yalcin, M. Sozbilir, C. Dogar, The investigation of adsorption thermodynamics and mechanism of a cationic surfactant, CTAB, onto powdered active carbon, *Fuel Process Technol.* 81 (2003) 57–66.
- [47] L. Cymbal, J. Greenleaf, D. Leun, A.K. Sen Gupta, Polymer supported inorganic nanoparticles: characterization and environmental applications, *React. Funct. Polym.* 54 (2003) 167–180.
- [48] E.R. Nightingale, Phenomenological theory of ion salvation, effective radii of hydrated ions, *J. Phys. Chem.* 63 (1959) 1381–1387.
- [49] I. Mobasherpour, E. Salahi, M. Pazouki, Comparative of the removal of Pb<sup>2+</sup>, Cd<sup>2+</sup> and Ni<sup>2+</sup> by nano crystallite hydroxyapatite from aqueous solutions: adsorption isotherm study, *Arab. J. Chem.* 5 (2012) 439–446.
- [50] S.A. Chaudhry, T.A. Khan, I. Ali, Adsorptive removal of Pb(II) and Zn(II) from water onto manganese oxide-coated sand: isotherm, thermodynamic and kinetic studies, *Egypt J. Basic Appl. Sci.* 3 (2016) 287–300.
- [51] B. Kepchayom, J. Wan, G. Zeng, D. Huang, W. Xue, L. Hu, C. Huang, C. Zhang, M. Cheng, Synthesis and application of magnetic chlorapatite nanoparticles for zinc (II), cadmium (II) and lead (II) removal from water solutions, *J. Colloid Interface Sci.* 505 (2017) 824–835.
- [52] L. Yuan, Y. Liu, Removal of Pb(II) and Zn(II) from aqueous solution by ceramite prepared by sintering bentonite, iron powder and activated carbon, *Chem. Eng. J.* 215 (2013) 432–439.
- [53] H. Cho, K. Wepasnick, B. Smith, F. Bangash, D. Fairbrother, W. Ball, Sorption of aqueous Zn(II) and Cd(II) by multiwall carbon nanotubes: the relative roles of oxygen-containing functional groups and graphenic carbon, *Langmuir* 26 (2009) 967–981.
- [54] A. Elham, T. Hossein, H. Mahnoosh, Removal of Zn(II) and Pb (II) ions using rice husk in food industrial wastewater, *J. Appl. Sci. Environ. Manage.* 14 (2010) 159–162.
- [55] T. Bohli, Comparative study of bivalent cationic metals adsorption Pb(II), Cd(II), Ni (II) and Cu(II) on olive stones chemically activated carbon, *J. Chem. Eng. Process Technol.* 4 (2013).
- [56] C. Chen, H. Liu, T. Chen, D. Chen, R. Frost, An insight into the removal of Pb(II), Cu (II), Co(II), Cd(II), Zn(II), Ag(I), Hg(I), Cr(VI) by Na(I)-montmorillonite and Ca(II)-montmorillonite, *Appl. Clay Sci.* 118 (2015) 239–247.
- [57] J.E. Efome, D. Rana, T. Matsuura, C.Q. Lan, Metal organic frameworks supported on nanofibers to remove heavy metals, *J. Mater. Chem. A* 6 (2018) 4550–4555.
- [58] I. Langmuir, The adsorption of gases on plane surfaces of glass, mica and platinum, *J. Am. Chem. Soc.* 40 (1918) 1361–1403.
- [59] T.W. Weber, R.K. Chakravot, Pore and solid diffusion models for fixed bed adsorbents, *AIChE J.* 20 (1974) 228–238.

- [60] A. Sari, M. Tuzen, D. Citak, M. Soylak, Equilibrium kinetic and thermodynamic studies of adsorption of Pb(II) from aqueous solution onto Turkish kaolinite clay, *J. Hazard. Mater.* 149 (2007) 283–291.
- [61] X.S. Wang, J. Huang, H.Q. Hua, J. Wang, Y. Qin, Determination of kinetic and equilibrium parameters of the batch adsorption of Ni(II) from aqueous solutions by Na-mordenite, *J. Hazard. Mater.* 142 (2007) 468–476.
- [62] H. Freundlich, Adsorption in solution, *Phys. Chem. Soc.* 40 (1906) 1361–1368.
- [63] M.J. Temkin, V. Phyzev, Recent modifications to Langmuir isotherms, *Acta Physicochim. URSS* 12 (1940) 217–222.
- [64] A. Sari, M. Tuzen, D. Citak, M. Soylak, Equilibrium, kinetic and thermodynamic studies of adsorption of Pb(II) from aqueous solution onto Turkish kaolinite clay, *J. Hazard. Mater.* 149 (2007) 283–291.
- [65] J. Li, C. Chen, Y. Zhao, J. Hu, D. Shao, X. Wang, Synthesis of water dispersible Fe<sub>3</sub>O<sub>4</sub>@ $\beta$ -cyclodextrin by plasma-induced grafting technique for pollutant treatment, *Chem. Eng. J.* 229 (2013) 296–303.
- [66] S. Lagergren, B.K. Svenska, Zurtheorie der sogenannten adsorption geloeisterstoffe *K Svenska, Vetenskapsakad Handl* 24 (1898) 1–39.
- [67] Y.S. Ho, Second order kinetic model for the sorption of cadmium onto tree fern: a comparison of linear and nonlinear methods, *Water Res.* 40 (2006) 119–125.
- [68] W.J. Weber, J.C. Morris, Equilibrium and capacities for adsorption on carbon, *J. Sanit. Eng. Division* 90 (1964) 79–91.
- [69] C. Sarici- Ozdemir, Y. Onal, Equilibrium, kinetic and thermodynamic adsorptions of the environmental pollutant tannic acid onto activated carbon, *Desalination* 251 (2010) 146–152.
- [70] A. Nilchi, R. Saberi, M. Moradi, H. Azizpour, R. Zarghami, Adsorption of cesium on copper hexacyanoferrate–PAN composite ion exchanger from aqueous solution, *J. Chem. Eng.* 172 (2011) 572–580.
- [71] N. Unlu, M. Ersoz, Removal of heavy metal ions by using dithiocarbamate – sporopollenin, *Sep. Purif. Technol.* 52 (2007) 461–469.
- [72] A.H. Bandegharai, M.S. Hosseini, Y.J. alalabadi, M. Sarwghadi, M. Nedaie, A. Taherian, A. Ghaznavi, A. Eftekhari, Removal of Hg (II) from aqueous solutions using a novel impregnated resin containing 1-(2-thiazolylazo)-2-naphthol (TAN), *J. Chem. Eng.* 168 (2011) 1163–1173.